Journal of Photochemistry & Photobiology, A: Chemistry 422 (2022) 113547

Contents lists available at ScienceDirect

Journal of Photochemistry & Photobiology, A: Chemistry

journal homepage: www.elsevier.com/locate/jphotochem

Exploration of silicon phthalocyanines as viable photocatalysts for organic transformations

Shelby D. Dickerson, Pooja J. Ayare, Aaron K. Vannucci, Sheryl L. Wiskur *

Department of Chemistry and Biochemistry, University of South Carolina, 631 Sumter St., Columbia, SC 29208, United States

ARTICLE INFO

Keywords:
Silicon Phthalocyanine
Photocatalysis
Singlet oxygen
Electron transfer
Organic photocatalyst
Energy transfer

ABSTRACT

Silicon phthalocyanines have been largely ignored as photocatalysts, despite their low energy excitation, long triplet lifetimes, and their ability to form singlet oxygen. By incorporating alkyl and silicon protecting groups as axial ligands on the silicon center, two silicon phthalocyanines have been generated with the goal of developing photocatalysts for organic synthesis. Using cyclic voltammetry and Stern Volmer quenching studies, we have shown silicon phthalocyanines are capable of electron transfer with appropriate substrates, including Hünig's base. We have also successfully used these catalysts in a reductive quenching reaction where Hünig's base served as a sacrificial electron donor in the reaction. In addition to being redox-active, our preliminary data also shows these compounds are capable of performing energy transfer reactions, by performing a reaction that utilizes singlet oxygen as a reactant under visible light conditions. This reaction, in combination with cyclic voltammetry studies, has also served as a model to understand how axial substitution on the silicon center seems to influence the photostability of these species.

1. Introduction

With relevance to cancer therapy [1], biomedical applications [2,3], and waste water treatment [4], photocatalysis has proven to be a powerful, versatile tool. Within the last fifteen years, synthetic chemists have increasingly employed photocatalysis, specifically using visible-light, for unique organic transformations, including photocycloadditions and C–H bond activations, just to name two [5,6,7,8,9]. Photocatalysts provide mild, sustainable pathways for reactions to occur by producing excited species that achieve intricate molecular transformations not always possible by established protocols or traditional reagents. For example, selective activation of vinyl halides to generate alkyl radicals has been a key goal in modern organic synthesis but has been difficult to achieve due to high reduction potentials [10]. However, common photocatalysts afford reduction potentials complementary to vinyl halides and allow new C–C bond forming routes under mild reaction conditions [11].

Many photocatalytic reactions are promoted by ruthenium- and iridium-based catalysts [8,12] because of their long-lived triplet state lifetimes and large redox properties; however, a push towards reducing the use of these precious metals has led to a growing interest in organic photocatalysts [13,14,15], such as Eosin Y [16,17,18,19] and derivatives [20], BODIPY derivatives [21], acridinium salts [22,23], Rose Bengal [24], and some newer amine heterocycles [25,26,27,28] just to name a few. Despite the rapid growth of organic photocatalysts there are still limitations that need to be overcome. For example, many of the organic photocatalysts are salts, therefore they have limited solubility in non-polar organic solvents. Additionally, there is a need to develop highly reducing catalysts that are competitive with ruthenium and iridium photocatalysts [13]. The focus of this study is to develop two axially-substituted silicon phthalocyanine organocatalysts that are soluble in a wide range of organic solvents and are competitive with ruthenium- and iridium-based photocatalysts. Silicon phthalocyanines are neutral compounds, where the substituents in the axial positions can alter their solubility, stability, and photophysical and photochemical properties. We found our silicon phthalocyanines are soluble in a range of solvents and possess redox potentials competitive with existing organic photocatalysis. These catalysts were successfully employed in an energy transfer reaction and redox reaction where the silicon phthalocyanines were competitive or out-performed the original organic photocatalysts under similar conditions.

Silicon phthalocyanines are porphyrin-based structures with phenyl rings fused on the porphyrin core and this class of compounds has great potential as visible-light mediated photocatalysts due to their ability to

* Corresponding author.
E-mail address: wiskur@mailbox.sc.edu (S.L. Wiskur).

https://doi.org/10.1016/j.jphotochem.2021.113547
Received 2 June 2021; Received in revised form 17 August 2021; Accepted 9 September 2021
Available online 13 September 2021
1010-6030/© 2021 Elsevier B.V. All rights reserved.

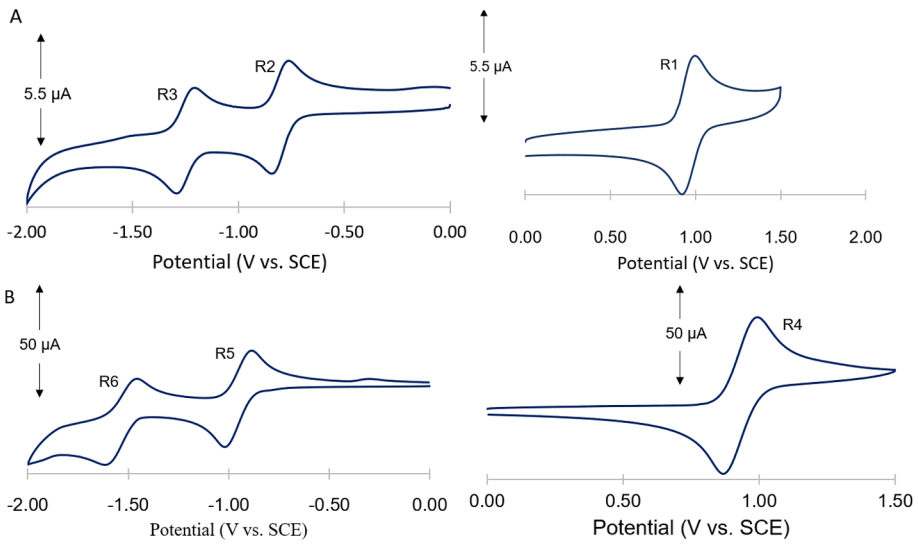

Fig. 1. Reduction (left) and oxidation (right) cyclic voltammetries of A. **1** at 1.7 mM and B. **2** at 2 mM at 0.1 Vs^{-1} in CH_2Cl_2/TBAH.

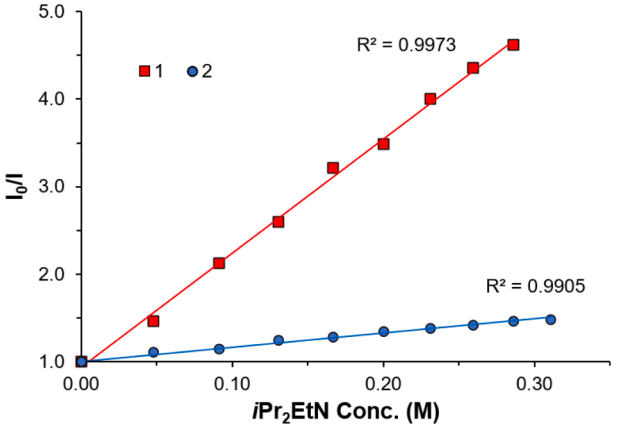

Fig. 2. Stern Volmer quenching studies of **1** (8 X 10^{-7} M) and **2** (3 X 10^{-7} M) with Hünig's base in chloroform. Catalysts **1** and **2** were excited at 675 nm and emission was collected from 630 to 800 nm. I_0 is in reference to 676.5 nm.

absorb long wavelengths and their high structural tunability [29]. The extended conjugation of these molecules allows for long wavelength absorption, usually varying in the red region (600–800 nm range) [30,31]. The energy absorbed promotes the compound into an excited state, which allows for one of two processes: energy transfer or electron transfer, the two most common pathways for photocatalysis to occur. Silicon phthalocyanines are known to participate in an energy transfer process when activated by light as shown by their use in photodynamic therapy [32]. When the excited molecule interacts with molecular oxygen, energy is transferred to produce highly reactive singlet oxygen, which reacts with cancer cells and initiates cell death [33,34]. While redox values for silicon phthalocyanines have been reported and are conducive for photoredox reactions [35,36,37], there are limited examples of their use in these reactions [38,39], i.e. the direct electron transfer from the photocatalyst to the substrate or a secondary catalyst to perform the desired catalytic reaction [40]. It is known that the photophysical and photochemical properties of silicon phthalocyanines can be modulated by substituting the compounds in various positions [41], but there is a lack of data showing how these changes affect electron transfer efficiency and stability/reversibility of electron transfer in organic reactions. Our research focused on variations in substitution in the axial position (R on **1** and **2**) and employing these catalysts in electron and energy transfer processes. The work herein analyzes how axially-substituting silicon phthalocyanines with pentyl (**1**) and trihexylsilyl groups (**2**) on the silicon center influence the redox stability and the photophysical and photochemical properties of the silicon phthalocyanines. The ability of the catalysts to promote two reactions were investigated: (1) an energy transfer cycloaddition reaction involving singlet oxygen and (2) an energy transfer dehalogenation reaction. Additionally, full characterization of the compounds was undertaken, including their electrochemical properties and their stabilities under these conditions.

2. Results and discussion

The synthesis and characterization of the silicon phthalocyanine catalysts were undertaken following literature procedures generating compounds that matched literature characterization. The synthesis of alkoxy substituted catalyst **1** followed the procedure outlined by Chen and coworkers, where deprotonated amyl alcohol displaced two chlorides on the silicon center of silicon phthalocyanine dichloride **3** with moderate yields (Scheme 1) [42]. The synthesis of the silyl protected catalyst **2** was adapted from Lessard et al. starting with the dihydroxyl silicon phthalocyanine **4** [18]. The hydroxyl groups were protected by reacting them with trihexylsilyl chloride to obtain **2** in 56% yield in one step (Scheme 1).

Voltammetric studies of pentyl catalyst (**1**) and trihexylsilyl catalyst (**2**) were carried out in dichloromethane with a 0.1 M tetrabutylammonium hexafluorophosphate ($TBAPF_6$) electrolyte. Fig. 1 shows the cyclic voltammograms (CVs) of **1** and **2**. Silicon phthalocyanine **1** exhibited one quasi-reversible oxidation process at $E_{1/2}$ = 0.95 V, labeled as R_1. Quasi-reversible is defined as having a cathodic to anodic peak current ($i_{p,c}/i_{p,a}$) at unity, but a peak to peak separation of greater than 100 mV. For the reductive scan, **1** exhibited two primarily irreversible reduction processes labeled as R_2 (E = -0.8 V) and R_3 (E = -1.2 V). As shown in the SI, the reduction waves for **1** do not follow the predicted linear dependence of peak current (i_p) on the square root of scan rate ($v^{1/2}$) that occurs for reversible redox processes. This lack of electrochemical reversibility of **1** indicates a lack of chemical stability upon reduction and is consistent with previous reports that show these class of silicon phthalocyanines complexes require extremely bulky axial groups to exhibit chemical stability [43,44].

Compound **2** does contain two, bulky trihexylsilyl groups at the axial position. The CVs of **2** show both a reversible oxidation (R_4, $E_{1/2}$ = 0.95 V, i_{pc}/i_{pa} = 1) and a reversible first reduction (R_5, $E_{1/2}$ = -0.93 V, i_{pc}/i_{pa} = 1) followed by a quasi-reversible second reduction (R_6, $E_{1/2}$ = -1.5 V

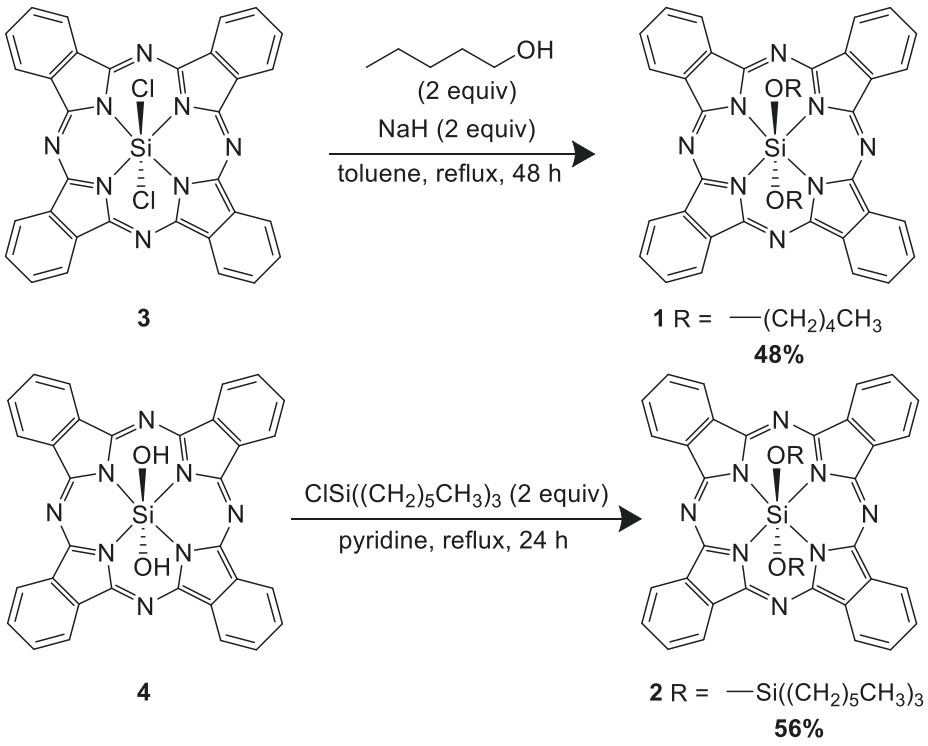

Scheme 1. Synthetic schemes for **1** and **2**.

Table 1
Ground state and excited state redox potentials of photocatalysts.

	$E_{1/2}^{ox}$ (V)	$E_{1/2}^{red}$ (V)	$E^*_{ox}(CAT^{\bullet+}/CAT^*)$ (V)	$E^*_{red}(CAT^*/CAT^{\bullet-})$ (V)
1	0.95	−0.8, −1.2	−0.89	1.04, 0.64
2	0.95	−0.93, −1.5	−0.895	0.915, 0.345
Eosin Y	0.78	−1.06	−1.11	0.83

$i_{pc}/i_{pa} < 1$). The CVs thus show that compound **2** is more stable towards redox processes and this stability can likely be attributed to the bulkier axial groups when compared to **1**. Stability of compounds while undergoing one-electron redox processes is an important attribute of photoredox catalysts. It is also worth noting that the electrochemistry reported here of **2** is consistent with previously reported data on this compound [19,45].

Absorption and emission profiles for **1** and **2** were also collected and shown in Figures S1-S4 in the SI. The absorbance spectra for silicon phthlocyanines commonly report distinctive Q band and Soret bands around 670–680 nm and 350 nm, respectively [28,46]. These bands refer to the transitions from the ground state to the first excited state (Q band) and from ground state to the second excited state (Soret band) [47]. The absorption profiles for **1** and **2** also exhibited Q and Soret bands near the expected wavelengths. Compounds **1** and **2** have Q bands and maximum absorptions (λ_{max}) at 672.5 nm and 669 nm with extinction coefficients (ε) of 1.01 × 10^5 $M^{-1}cm^{-1}$ and 3.16 × 10^5 $M^{-1}cm^{-1}$, respectively, and Soret bands around 355 nm for **1** and 358 nm for **2** [26,48]. The emission peaks for **1** and **2** (676.5 nm for both) showed Stokes shifts of 4 nm and 7.5 nm, respectively when excited at 670 nm.

Since photochemistry primarily occurs in the triplet state of silicon phthalocyanines, the excited state redox potentials were calculated to

Table 2
The [2 + 4]-cycloaddition of pyridone **5** to *endo*-peroxide **6.**

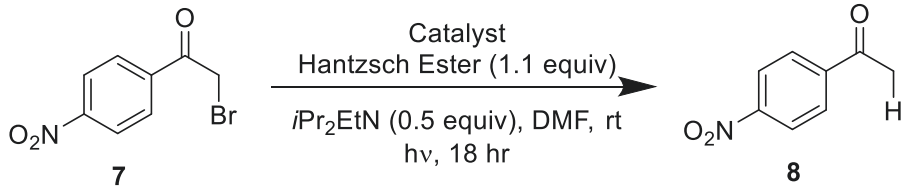

Entry[a]	Catalyst:	Time	Light Source/Wattage	Isolated Yields (%)
1	**1**	18 h	LED/100	25
2	**2**	18 h	LED/100	67
3	**TPP**	18 h	LED/100	36
4[b]	**TPP**	45 min	Sodium Vapor Lamp/800	97

[a] All reactions were performed at 0.11 M concentration with respect to **5** in toluene at −78 °C for 18 h.
[b] Literature conditions from reference [51].

accurately determine the redox potentials used for catalysis. Therefore equations S1 and S2 [14] (see SI) were used to find the excited state potentials where E^*_{red} depicts the excited state reduction potential and E^*_{ox} is the excited state oxidation potential. Table 1 includes the excited state potentials of our catalysts and Eosin Y for comparison [49]. Compared to Eosin Y, our silicon phthalocyanines offer a lower excited oxidation potential, but a larger range of excited reduction potentials when considering all reduction potentials.

The ability of photocatalysts **1** and **2** to be reductively quenched by Hünig's base, a commonly used sacrificial electron donor, was then explored with fluorescence quenching and a Stern-Volmer analysis. Fig. 2 compares the quenching of **1** and **2** by Hünig's base where the linear correlation is indicative of effective electron transfer from Hünig's base to the excited-state pentyl **1** and trihexylsilyl **2** species presumably through dynamic quenching [23]. The increased slope for **1** compared to **2**, indicates faster electron transfer kinetics, which is an advantageous property of photoredox catalysts.

Next, the ability for photocatalysts **1** and **2** to promote an energy transfer reaction was investigated and compared to a literature standard (Table 2) [50]. The photocatalytic reaction chosen was a [2 + 4]-cycloaddition of singlet oxygen with pyridine-2(1*H*)-one (**5**) to form *endo*-peroxide **6**. During the reaction, the excited photocatalyst transfers energy to molecular oxygen to form singlet oxygen which reacts with the diene of **5** [51]. We chose to promote the reaction via a 100 W, white LED light bulb, which is an affordable, readily available light source that fits the absorbance range of both **1** and **2**. Both silicon phthalocyanine catalysts promoted the formation of **6** using conditions similar to the literature [25], but with a lower intensity light source (Table 2, entries 1 and 2). Trihexylsilyl catalyst **2** provided higher yields compared to pentyl catalyst **1.** We believe the low yields with **1** were a result of catalyst decomposition during the reaction, due to the inability to recover the catalyst during work up. This result is consistent with the irreversible redox properties discovered in the cyclic voltammetry studies shown in Fig. 1. Therefore, we believe the bulkiness of the trihexylsilyl group on **2** is important in the overall stability of these structures. Bach and coworkers had originally employed the photocatalyst tetraphenylporphyrin (TPP) and an 800 W sodium vapor lamp, resulting in significantly higher yields than our catalysts in less time (Entry 4). Employing TPP as the catalyst with the LED light source, resulted in a significant drop in yield to 36% (Entry 3), which is also dramatically lower than the yield with catalyst **2**. This suggests that **2** does a better job of activating oxygen versus TPP with this simple light source.

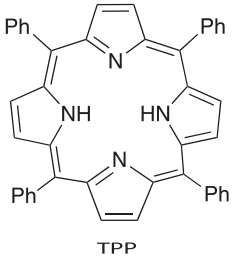

TPP

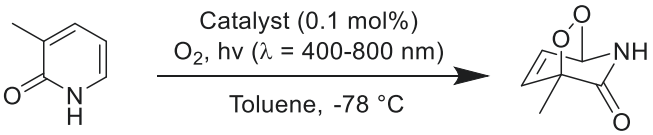

5 **6**

The photocatalysts **1** and **2** were then examined in a photoredox catalysis reaction, specifically a reductive dehalogenation reaction (Table 3) [52]. This reaction was chosen to compare the performance of our organic photocatalysts against the popular Eosin Y catalyst, again using a commercially-available LED bulb with the literature's reaction conditions. The excited photocatalyst accepts an electron by reducing **7** and breaking the bromine-carbon bond to produce an electron-deficient radical on the α-carbon, which picks up a hydrogen radical to form **8** [52]. We believe pentyl catalyst (**1**) resulted in no yield due to instability of **1**. Once the reaction was completed, we were unable to recover the catalyst. We believe this lack of stability suggests the solvent is possibly interacting with **1**, or the light source was too high energy and **1** decomposed during the reaction. Trihexylsilyl catalyst **2** successfully promoted the reaction with just under 40% yield (entry 2). This is lower than the literature yield of 83% with Eosin Y and a different light source (entry 11). We also noticed while performing the reaction with trihexylsilyl catalyst **2**, that the solution was dark black in color, suggesting that the reaction was too concentrated for the light to penetrate, limiting the amount of catalyst being excited. Therefore, we diluted the reaction to 1.25 mM (with respect to the catalyst) and the yield increased to 59% (entry 3), closing the gap in yield with published Eosin Y results (entry 11). The literature utilized a blue LED light source, which is optimal for Eosin Y, and we again wanted a more representative comparison using Eosin Y with our 100 W, white LED bulb (entry 10). The light source

Table 3
Dehalogenation reaction.

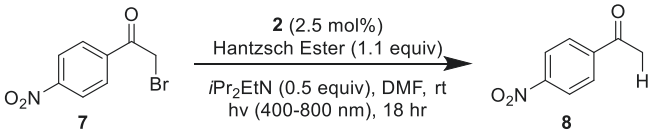

7 0.443 g **8**

Entry[a]	Catalyst	Catalyst (mM)	LED Light Source	Solvent	Yield (%)
1	**1**	6.25	White	DMF	0
2	**2**	6.25	White	DMF	38
3	**2**	1.25	White	DMF	59
4	**1**	1.25	Red	DMF	25
5	**2**	1.25	Red	DMF	27
6	**1**	1.25	Red	Chloroform	31
7	**2**	1.25	Red	Chloroform	22
8	**1**	1.25	White	Chloroform	31
9	**2**	1.26	White	Chloroform	21
10	Eosin Y	6.25	White	DMF	55
11[b]	Eosin Y	6.25	Blue	DMF	83

[a] All reactions were performed at 0.05 M concentration with respect to **7** in specified solvent at room temperature for 18 h using specified LED light source.
[b] Literature conditions from reference [52].

Table 4
Large scale of dehalogenation reaction and catalyst stability study.

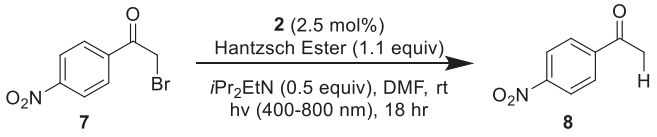

7 0.443 g **8**

Entry[a]	% Yield	% Recovered Catalyst
1	53	100
2	55	100
3	64	76

[a] All reactions were performed at 0.05 M concentration with respect to **7** in specified solvent at room temperature for 18 hr using specified LED light source, recycling the same sample of **2**.

decreased Eosin Y's yield (entry 10) and resulted in a similar yield compared to our catalyst **2** (entry 3). Since catalysts **1** and **2** absorb red light between ~600–700 nm (see Supporting information for spectra), with a maximum at 675 nm, we employed a commercially-available red LED source to investigate the effect on the reaction (entries 4 and 5). To our surprise, under these conditions, catalyst **1** generated 25% product. We contributed this new reactivity to less degradation of catalyst **1** with the less intense red LEDs compared to our white LED (a comparison of 24 W to 100 W). Catalyst **2** had a decrease in yield (entry 5) with the red light compared to the white LED (entry 3), and we again attribute this to the lower wattage light source.

Since our CV studies showed reversible reductions for both **1** and **2** in chloroform and we were concerned that DMF could be reacting with our catalysts, the dehalogenation reaction was run in chloroform with both catalysts (Table 3, entries 6–9). Both the red and the white LED light sources were employed, showing a slight increase in product with catalyst **1** over DMF with no difference between the two light sources in chloroform (31% yield, entries 6 and 8). Catalyst **2** resulted in a decrease in yield versus reactions run in DMF, again resulting in the same yield regardless of the light source (entries 7 and 9). The redox potentials of **1** and **2** suggest they should have similar reactivity, but solvent and the wattage of the light source can have a negative effect on these catalysts, especially **1**, since there is evidence that it is less stable. Changing the solvent from DMF, increased the yield of **1** but had a negative effect on catalyst **2**. DMF is used exclusively in the literature for this reaction, suggesting it could have a stabilizing effect on the reaction intermediates.

Finally, we performed a large-scale reaction with catalyst **2** as well as a catalyst recyclability study. The goal was to recycle the catalyst over three reactions to determine stability, starting with close to half a gram of starting material. Table 4 shows the yield of the reaction does not decrease with the scale up nor does it change if the catalyst is recycled, suggesting **2** is stable to undergo the electron transfer for several cycles for the first two reactions. Entry 3 showed that while the yield is not affected, we did start to see decomposition of **2** since less was recovered from the reaction.

3. Conclusion

In conclusion, silicon phthalocyanines are viable options for photocatalysis. We have shown silicon phthalocyanines are able to undergo electron and energy transfer processes competitive with existing photocatalysts. The redox potentials of our silicon phthalocyanines are competitive with known organocatalysts, such as Eosin Y. Future studies should focus on the stabilization on the silicon center as well as how manipulating the peripheral sites would enhance the redox properties of the silicon phthalocyanines.

4. Experimental section

4.1. General remarks

All reactions were carried out under a N_2 atmosphere using oven dried glassware. Amyl alcohol and pyridine were distilled prior to use. Toluene was dried by passing through a column of activated alumina before use and stored over molecular sieves. All other solvents and chemicals were obtained from commercial sources and used without further purification. Flash column chromatography was performed on silica gel (32–63 microns). ^{1}H NMR spectra were recorded on a Bruker Avance III (400 or 300 MHz). Chemical shifts are reported in ppm with TMS or chloroform as an internal standard (TMS 0.00 ppm for ^{1}H and ^{13}C or $CHCl_3$ 7.26 ppm and 77.16 for ^{1}H and ^{13}C, respectively). ^{13}C NMR spectra were recorded on a Bruker Avance III (101 or 75 MHz) with complete proton decoupling. The data reported for ^{1}H NMR are as follows: chemical shift, multiplicity (s = singlet, d = doublet, t = triplet, q = quartet, dd = doublet of doublet, td = triplet of doublets, dt = doublet of triplet, sept = septet, m = multiplet). Steady-state emission spectra were acquired on an Edinburgh FS5 fluorescence spectrometer equipped with a 150 W Continuous Wave Xenon Lamp source for excitation. Absorbance scans were taken on a Shimadzu UV-2600 UV-Vis Spectrophotomer using 1 cm quartz cuvette at 25 °C. Cyclic voltammetry (CV) performed on a CH Instruments 601D potentiostat with a 3 mm diameter glassy carbon working electrode, a Pt wire (99.99%) counter electrode, and a saturated calomel electrode (SCE). The glassy carbon electrode was manually prepared by polishing the surface with a 0.05 μm alumnia suspension. Solutions for electrochemical characterization contained 100 mM tetrabutylammonium hexfluorophosphate ($TBAPF_6$) which was further purified by recrystallization in ethanol and dried under vacuum at 80 °C over 24 hours. Dichloromethane was purged with N_2 prior to any measurements taken and between measurements.

4.2. Bis-pentyloxy silicon phthalocyanine (1)

The synthesis of **1** was adapted from the literature [20]. In a flame-dried four-dram vial equipped with a stir bar, sodium hydride (2 equiv, 0.33 mmol) was added under nitrogen and washed with pentane (3 X 5 mL). Amyl alcohol (2 equiv, 0.33 mmol) was added to the vial with sodium hydride, and the solution stirred in 3 mL of dry toluene for 15 minutes. The solution was then added to a 50 mL round bottom flask with **3** (1 equiv, 0.165 mmol) and a stir bar under nitrogen. The mixture was diluted with 12 mL of dry toluene and refluxed overnight under nitrogen. The mixture was then concentrated via rotary evaporation and filtered with cold chloroform. The filtrate was collected and concentrated via rotary evaporation to afford **1** as a dark blue solid without further purification. Yield: 48%. ^{1}H NMR (300 MHz, $CDCl_3$) δ (ppm): 9.658 (m, 8 H), 8.352 (m, 8 H), -0.117 (t, J = 15.1 Hz, 6 H), -0.377 (m, 4 H), -1.401 (m, 4 H), -1.677 (m, 4 H).

4.3. Bis(tri-n-hexylsiloxy)-silicon phthalocyanine (2)

The synthesis of **2** was adapted from the literature [18]. To a flame-dried 5 mL round bottom flask equipped with a stir bar, under nitrogen was added **4** (1 equiv, 0.072 mmol), trihexylsilylchoride (2 equiv, 0.145 mmol), and 2.5 mL of distilled pyridine. A reflux condenser was added, and the mixture refluxed for 48 hours under nitrogen. The reaction was then concentrated via rotary evaporation and the resulting blue solid was purified by column chromatography (silica gel, 1% $CHCl_3$/hexane) to give **2** as a blue solid. Yield: 56%. ^{1}H NMR (300 MHz, $CDCl_3$) δ (ppm): 9.656 (m, 8 H), 8.335 (m, 8 H), 0.850 (m, 12 H), 0.731 (t, J = 6.6 Hz, 18 H), 0.383 (m, 12 H), 0.043 (m, 12 H), -1.26 (m, 12H), -2.421 (m, 12 H).

4.4. Synthesis of endoperoxide *6* - General photocatalytic procedure

The synthesis of endoperoxide **6** was adapted from the literature [23]. In a flame-dried four-dram vial equipped with a stir bar, pyridone **5** (1 equiv, 1.4 mmol) was added with 0.1 mol% of photocatalyst and 10 mL of dry toluene under nitrogen and then sealed with a septa vial cap. The solution was then bubbled with oxygen and placed in a -78 °C bath for 18 hours and irradiated by a 100 W LED lamp. The solution was then warmed to room temperature, and the solid was filtered and washed with diethyl ether. The combined organic layers were dried over $NaSO_4$, filtered, and concentrated via rotary evaporation. The solid was collected without further purification to afford endoperoxide **6**. ^{1}H NMR (300 MHz, $CDCl_3$) δ (ppm): 6.864 (dd, 5.46 Hz, 7.90 Hz, 1 H), 6.497 (dd, J = 1.8 Hz, 7.9 Hz, 1 H), 5.764 (td, J = 1.70 Hz, J = 5.27 Hz, 1 H), 1.645 (s, 3 H).

4.5. Reductive dehalogenation of α-halogenated carbonyl *8* - General photocatalytic procedure

The synthesis of **8** was adapted from the literature [24]. In a flame-dried four-dram vial equipped with a stir bar, **7** (1 equiv, 0.5 mmol) was

added under nitrogen. DMF (10 mL), Hünig's base (2 equiv, 1 mmoL), Hantzsch ester (1.1 equiv, 0.55 mmol), and photocatalyst (1.25 mM, 0.0125 mmol) were added under nitrogen to the vial and sealed with a septa vial cap. The solution was degassed by "freeze- pump-thaw" cycles (x3) via syringe needle. The vial was then irradiated by a 100 W LED lamp for 18 hours at room temperature. The reaction was then diluted with diethyl ether, washed (3x) with water and the water layer was washed (2x) with diethyl ether. The combined organic layers were dried over $NaSO_4$, filtered, and concentrated via rotary evaporation. Purification of **8** was achieved by column chromatography (silica gel, 25% Et_2O/hexanes). ^1H NMR (300 MHz, $CDCl_3$) δ (ppm): 8.337 (d, $J = 8.8$ Hz, 2 H), 8.133 (d, $J = 8.8$ Hz, 2 H), 2.702 (s, 3 H).

CRediT authorship contribution statement

Shelby D. Dickerson: Investigation, Formal analysis, Visualization, Writing - original draft. **Pooja J. Ayare:** Supervision. **Aaron K. Vannucci:** Validation, Resources, Formal analysis, Supervision, Writing - review & editing. **Sheryl L. Wiskur:** Conceptualization, Funding acquisition, Writing - review & editing.

Declaration of Competing Interest

The authors declare that they have no known competing financial interests or personal relationships that could have appeared to influence the work reported in this paper.

Acknowledgement

We gratefully acknowledge support from the University of South Carolina for funding for the SPARC grant and the ASPIRE grant. We also acknowledge support from NSF Award ID 1856772. We would also like to thank Dr. Natalia Shustova's group, specifically Derek Williams, Katya Dolgopolova, and Corey Martin for help with obtaining spectra, and Mevan Dissanayake from Dr. Aaron Vannucci's group for help with obtaining CVs.

Appendix A. Supplementary data

Supplementary data to this article can be found online at https://doi.org/10.1016/j.jphotochem.2021.113547.

References

[1] Y. Zhu, J. Chen, S. Kaskel, Porphyrin-based metal-organic frameworks for biomedical applications, Angew. Chem. Int. Ed. 59 (2020) 2–28.
[2] W. Tomal, J. Ortyl, Soluble photoinitiators in biomedical applications, Polymers 12 (2020) 1–31.
[3] A.C. Mecha, M.N. Chollom, Photocatalytic ozonation of wastewater: a review, Environ. Chem. Lett. 18 (2020) 1491–1507.
[4] D. Petzold, M. Giedyk, A. Chatterjee, B. König, A retrosynthetic approach for photocatalysis, Eur. J. Org. Chem. 2020 (10) (2020) 1193–1244.
[5] C. Michelin, N. Hoffmann, Photosensitization and photocatalysis - perspectives in organic synthesis, ACS Catal. 8 (12) (2018) 12046–12055.
[6] M. Fagnoni, D. Dondi, D. Ravelli, A. Albini, Photocatalysis for the formation of the C-C bond, Chem. Rev. 107 (6) (2007) 2725–2756.
[7] C.K. Prier, D.A. Rankic, D.W.C. MacMillan, Visible light photoredox catalysis with transition metal complexes: applications in organic synthesis, Chem. Rev. 113 (7) (2013) 5322–5363.
[8] J.W. Tucker, C.R.J. Stephenson, Shining light on photoredox catalysis: theory and synthetic applications, J. Org. Chem. 77 (4) (2012) 1617–1622.
[9] B. Branchi, C. Galli, P. Gentili, Reactivity of aryl and vinyl radicals: abstraction of hydrogen atom or reaction with a nucleophile, Eur. J. Org. Chem. 2002 (16) (2002) 2844.
[10] S.K. Pagire, T. Föll, O. Reiser, Shining visible light on vinyl halides: expanding the horizons of photocatalysis, ACS Appl. Mater. Interfaces 53 (2020) 782–791.
[11] B.M. Hockin, C. Li, N. Robertson, E. Zysman-Colman, Photoredox catalysts based on earth-abundant metal complexes, Catal. Sci. Technol. 9 (2019) 889–915.
[12] N.A. Romero, D.A. Nicewicz, Organic photoredox catalysis, Chem. Rev. 116 (2016) 10075–10166.
[13] A. Vega-Peñaloza, J. Mateos, X. Companyó, M. Escudero-Casao, L. Dell'Amico, A Rational approach to organo-photocatalysis: novel designs and structure-property relationships, Angew. Chem. Int. Ed. 60 (3) (2021) 1082–1097.
[14] I.K. Sideri, E. Voutyritsa, C.G. Kokotos, Photoorganocatalysis, small organic molecules and light in the service of organic synthesis: the awakening of a sleeping giant, Org. Biomol. Chem. 16 (25) (2018) 4596–4614.
[15] D.M. Yan, J.R. Chen, W.J. Xiao, New roles for photoexcited eosin Y in photochemical reactions, Angew. Chem. Int. Ed. 58 (2019) 378–380.
[16] V. Srivastava, P.P. Singh, Eosin Y catalysed photoredox synthesis: a review, RSC Adv. 7 (50) (2017) 31377–31392.
[17] D.P. Hari, B. König, Synthetic applications of eosin Y in photoredox catalysis, Chem. Commun. 50 (51) (2014) 6688–6699.
[18] P. De Bonfils, L. Péault, P. Nun, V. Coeffard, State of the art of bodipy-based photocatalysts in organic synthesis, Eur. J. Org. Chem. 2021 (12) (2021) 1809–1824.
[19] M.V. Bobo, A.M. Arcidiacono, P.J. Ayare, J.C. Reed, M.R. Helton, T.N. Ngo, K. Hanson, A.K. Vannucci, A series of green light absorbing organic photosensitizers capable of oxidative quenching photocatalysis, ChemPhotoChem. 4 (2020) 1–8.
[20] J. Zhao, K. Xu, W. Yang, Z. Wang, F. Zhong, The triplet excited state of bodipy: formation. Modulation and application, Chem. Soc. Rev. 44 (2015) 8904–8939.
[21] A. Johsi-Pangu, F. Lèvesque, G.H. Roth, S.F. Oliver, L. Campeau, D. Nicewicz, D. A. DiRocco, Acridinium-based photocatalysis: A sustainable option in photoredox catalysis, J. Org. Chem. 7244–7249 (2016).
[22] B. Zilate, C. Fischer, C. Sparr, Design and application of aminoacridinium organophotoredox catalysts, Chem. Commun. (2020) 1767.
[23] S. Sharma, A. Sharma, Recent advances in photocatalytic manipulations of rose bengal in organic synthesis, Org. Biomol. Chem. 17 (2019) 4384–4405.
[24] T. Le, L. Galmiche, G. Masson, C. Allain, P. Audebert, A straightforward synthesis of a new family of molecules: 2,5,8-trialkoxyheptazines. Application to photoredox catalyzed transformations, Chem. Commun. 56 (73) (2020) 10742–10745.
[25] T. Le, T. Courant, J. Merad, C. Allain, P. Audebert, G. Masson, s-Tetrazine dyes: A facile generation of photoredox organocatalysts for routine oxidations, J. Org. Chem. 84 (24) (2019) 16139–16146.
[26] E.J. Rabe, K.L. Corp, X. Huang, J. Ehrmaier, R.G. Flores, S.L. Estes, A. L. Sobolewski, W. Domcke, C.W. Schlenker, Barrierless heptazine-driven excited state proton-coupled electron transfer: implications for controlling photochemistry of carbon nitrides and aza-arenes, J. Phys. Chem. C. 123 (49) (2019) 29580–29588.
[27] R. Saritha, S.B. Annes, S. Ramesh, Metal-free, regioselective, visible light activation of 4CzIPN for the arylation of 2*H*-indazole derivatives, RSC Adv. 11 (23) (2021) 14079–14084.
[28] K. Mitra, M.C.T. Hartman, Silicon Phthalocyanines: synthesis and resurgent applications, Org. Biomol. Chem. 19 (2021) 1168–1190.
[29] M. Liu, C. Li, ChemPlusChem. 85 (2020) 948–957.
[30] T.M. Grant, D.S. Josey, K.L. Sampson, T. Mudigonda, T.P. Bender, B.H. Lessard, Chem. Rec. 19 (2019) 1093–1112.
[31] E.D. Baron, C.L. Malbasa, D. Santo-Domingo, P. Fu, J.D. Miller, K.K. Hanneman, A. H. Hsia, N.L. Oleinick, V.C. Colussi, K.D. Cooper, Silicon phthalocyanine (Pc 4) photodynamic therapy is a safe modality for cutaneous neoplasms: results of a phase 1 clinical trial, Lasers Surg. Med. 42 (2010) 888–895.
[32] X. Chen, Q. Guo, S. Dong, J. Chen, S. Xie, D. Ma, L. Chen, H. Yang, Y. Huang, Y. Peng, Distribution, trafficking, and in vitro photodynamic therapy efficacy of cholesterol silicon(IV) phthalocyanine and its nanoparticles in breast cancer cells, ACS Appl. Bio Mater. 2 (2019) 5976–5984.
[33] P. Sen, T. Nyokong, A novel axially palladium(II)-schiff base complex substituted silicon(IV) Phthalocyanine: Synthesis, Characterization, photophysicochemical properties and photodynamic antimicrobial chemotherapy activity against Staphylococcus Aureus, Polyhedron. 173 (2019), 114135.
[34] B.H. Lessard, J.D. Dang, T.M. Grant, D. Gao, D.S. Seferos, T.P. Bender, Bis(Tri- n -hexylsilyl oxide) silicon phthalocyanine: A unique additive in ternary bulk heterojunction organic photovoltaic devices, ACS Appl. Mater. Interfaces. 6 (2014) 15040–15051.
[35] J.-P. Daziano, S. Steenken, C. Chabannon, P. Mannoni, M. Chanon, M. Julliard, Photophysical and redox properties of a series of phthalocyanines: relation with their photodynamic activities on *TF-1* and daudi leukemic, Cells 64 (1996) 712–719.
[36] Z. Li, M. Lieberman, Axial reactivity of soluble silicon(IV) phthalocyanines, Inorg. Chem. 40 (5) (2001) 932–939.
[37] J. Huang, Y. Wu, D. Wang, Y. Ma, Z. Yue, Y. Lu, M. Zhang, Z. Zhang, P. Yang, Silicon Phthalocyanine covalently functionalized n-doped ultrasmall reduced graphene oxide decorated with Pt nanoparticles for hydorgen evolution from water, ACS Appl. Mater. Interfaces. 3732–3741 (2015).
[38] B. Xiao, M. Zhu, X. Li, P. Yang, L. Qiu, C. Lu, A stable and efficient photocatalytic hydrogen evolution system based on covalently linked silicon-phthalocyanine-graphene with surfactant, Int. J. Hydrog. Energy. 41 (27) (2016) 11537–11546.
[39] M. Shaw, J. Twilton, D.W.C. MacMillan, Photoredox catalysis in organic chemistry, J. Org. Chem. 81 (2016) 6898–6926.
[40] J.C. Koziar, D.O. Cowan, Photochemical heavy-atom effects, Acc. Chem. Res. 11 (1978) 334–341.
[41] X. Chen, D. Ma, K. Cai, S. Pan, Effect of axial ligands on the photophysical properties of new silicon (IV), Phthalocyanines 68 (2015) 732–740.
[42] Z. Biyiklioglu, H. Bas, Synthesis and electrochemistry of non-aggregated axially disubstituted silicon phthalocyanines bearing benzoxazine substituents, Inorg. Chim. Acta 427 (2015) 293–298.

[43] D. Demirkapi, A. Sirin, B. Turanli-Yildiz, Z.P. Cakar, B.S. Sesalan, The synthesis of new silicon phthalocyanines and analysis of their photochemical and biological properties, Synth. Met. 187 (2014) 152–159.
[44] H. Baş, Z. Biyiklioglu, Non-aggregated axially naphthoxazin group substituted silicon phthalocyanines: synthesis and electrochemistry, J. Organomet. Chem. 791 (2015) 238–243.
[45] O.M. Opeyemi, H. Louis, C.I. Opara, O.F. Oyebanji, T.O. Magu, Adv J Chem A 2 (2019) 21–44.
[46] D. LeGourrièrec, M. Andersson, J. Davidsson, E. Mukhtar, L. Sun, L. Hammarstrom, J. Phys. Chem. A (1999) 557–559.
[47] B.L. Wheeler, G. Nagasubramanian, A.J. Bard, L.A. Schechtman, D.R. Dininny, M. E. Kenney, A silicon phthalocyanine and a silicon napthalocyanine: synthesis, electrochemistry, and electrogenerated chemiluminescence, J. Am. Chem. Soc. 106 (1984) 7404–7410.
[48] A.-W.-H. Mau, O. Johansen, W.H.F. Sasse, Xanthene dyes as sensitizers for the photoreduction of water, Photochem. Photobiol. 41 (1985) 503–509.
[49] C. Wiegand, E. Herdtweck, T. Bach, Enantioselectivity in visible light-induced, singlet oxygen [2+4] cycloaddition reactions (Type II photooxygenations) of 2-pyridones, Chem. Commun. 48 (2012) 10195–10197.
[50] T. Bach, H. Bergmann, K. Harms, Enantioselective intramolecular [2‡2]-photocycloaddition reactions in solution, Angew. Chem. Int. Ed. 39 (2000) 2302–2304.
[51] M. Neumann, S. Füldner, B. König, K. Zeitler, Metal-free, cooperative asymmetric organophotoredox catalysis with visible light, Angew. Chem. Int. Ed. 50 (2011) 951–954.
[52] J.M.R. Narayanam, J.W. Tucker, C.R.J. Stephenson, Electron-transfer photoredox catalysis: development of a tin-free reductive dehalogenation reaction, J. Am. Chem. Soc. 131 (2009) 8756–8757.